

Loss-of-Function Mutations in *APPL1* in Familial Diabetes Mellitus

Sabrina Prudente,^{1,*} Prapaporn Jungtrakoon,^{2,3} Antonella Marucci,⁴ Ornella Ludovico,⁴ Patinut Buranasupkajorn,^{2,3} Tommaso Mazza,¹ Timothy Hastings,² Teresa Milano,⁵ Eleonora Morini,⁴ Luana Mercuri,¹ Diego Bailetti,^{1,6} Christine Mendonca,² Federica Alberico,¹ Giorgio Basile,^{1,6} Marta Romani,¹ Elide Miccinilli,¹ Antonio Pizzuti,^{1,6} Massimo Carella,⁷ Fabrizio Barbetti,^{8,9} Stefano Pascarella,⁵ Piero Marchetti,¹⁰ Vincenzo Trischitta,^{1,4,6} Rosa Di Paola,⁴ and Alessandro Doria^{2,3,*}

Diabetes mellitus is a highly heterogeneous disorder encompassing several distinct forms with different clinical manifestations including a wide spectrum of age at onset. Despite many advances, the causal genetic defect remains unknown for many subtypes of the disease, including some of those forms with an apparent Mendelian mode of inheritance. Here we report two loss-of-function mutations (c.1655T>A [p.Leu552*] and c.280G>A [p.Asp94Asn]) in the gene for the Adaptor Protein, Phosphotyrosine Interaction, PH domain, and leucine zipper containing 1 (*APPL1*) that were identified by means of whole-exome sequencing in two large families with a high prevalence of diabetes not due to mutations in known genes involved in maturity onset diabetes of the young (MODY). *APPL1* binds to *AKT2*, a key molecule in the insulin signaling pathway, thereby enhancing insulin-induced *AKT2* activation and downstream signaling leading to insulin action and secretion. Both mutations cause *APPL1* loss of function. The p.Leu552* alteration totally abolishes *APPL1* protein expression in HepG2 transfected cells and the p.Asp94Asn alteration causes significant reduction in the enhancement of the insulin-stimulated *AKT2* and *GSK3β* phosphorylation that is observed after wild-type *APPL1* transfection. These findings—linking *APPL1* mutations to familial forms of diabetes—reaffirm the critical role of *APPL1* in glucose homeostasis.

Diabetes mellitus (DM [MIM: 125853]) is the most common metabolic disorder, imposing a worldwide burden on morbidity and mortality arising from its chronic complications.¹ Rather than being a single disorder, DM encompasses several distinct forms characterized by different clinical manifestations including a wide spectrum of age at onset.² Such clinical heterogeneity is paralleled by a marked genetic heterogeneity. Several disease genes have been identified for some monogenic forms of the disease such as “maturity-onset diabetes of the young” (MODY [MIM: 606391]) and neonatal diabetes (ND [MIM: 606176]).^{2,3} However, despite these advances, the causal genetic defect remains unknown for many subtypes of the disease, including some of the forms with an apparent Mendelian mode of inheritance. Filling this knowledge gap would be extremely useful because it would allow the development of predicting tools as well as novel treatments tailored to specific etiological mechanisms. During the past few years, whole-exome sequencing (WES), made possible by the advent of “next-generation” array-based sequencing methods, has emerged as a powerful and cost-effective strategy to achieve this goal.⁴

Here we describe two loss-of-function mutations in the gene for the Adaptor Protein, Phosphotyrosine Interaction, PH domain, and leucine zipper containing 1 (*APPL1*

[MIM: 604299]) that were identified through the WES approach in two large families with a high prevalence of diabetes not due to mutations in known MODY genes^{5,6} (S. Prudente et al., 2014, American Diabetes Association, 74th Scientific Sessions, abstract). WES was performed in 60 families (52 from the US and 8 from Italy) selected on the basis of the following criteria: (1) presence of overt diabetes in at least three consecutive generations with an apparent dominant transmission, (2) a proband and at least one first-degree relative with diabetes diagnosed before age 35, (3) diabetes entering the family from only one side, and (4) lack of mutations in the six most common MODY genes⁷ (*HNF4A* [MIM: 600281], *GCK* [MIM: 138079], *HNF1A* [MIM: 142410], *PDX1* [MIM: 600733], *HNF1B* [MIM: 189907], and *NEUROD1* [MIM: 601724]) as determined by Sanger sequencing. Study protocols and informed consent procedures were approved by the local Institutional Ethic Committees in Italy and the US and all participants gave written consent. This study was carried out in accordance with the Declaration of Helsinki, as revised in 2000. Family members were classified as having diabetes, pre-diabetes, or normal glucose tolerance based on the ADA 2014 criteria. For each family, WES was carried out in the proband and an additional diabetic member (both with age of disease onset <35 years) using

¹Mendel Laboratory, IRCCS Casa Sollievo della Sofferenza, 71013 San Giovanni Rotondo, Italy; ²Research Division, Joslin Diabetes Center, Boston, MA 02215, USA; ³Department of Medicine, Harvard Medical School, Boston, MA 02115, USA; ⁴Research Unit of Diabetes and Endocrine Diseases, IRCCS Casa Sollievo della Sofferenza, 71013 San Giovanni Rotondo, Italy; ⁵Department of Biochemical Sciences, Sapienza University, 00185 Rome, Italy; ⁶Department of Experimental Medicine, Sapienza University, 00161 Rome, Italy; ⁷Unit of Medical Genetics, IRCCS Casa Sollievo della Sofferenza, 71013 San Giovanni Rotondo, Italy; ⁸Laboratory of Mendelian Diabetes, Bambino Gesù Children’s Hospital, 00165 Rome, Italy; ⁹Department of Experimental Medicine and Surgery, University of Tor Vergata, 00133 Rome, Italy; ¹⁰Department of Clinical and Experimental Medicine, University of Pisa, 56127 Pisa, Italy

*Correspondence: s.prudente@css-mendel.it (S.P.), alessandro.doria@joslin.harvard.edu (A.D.)

<http://dx.doi.org/10.1016/j.ajhg.2015.05.011>. ©2015 by The American Society of Human Genetics. All rights reserved.

Table 1. Clinical and Genetic Characteristics of Examined Members from the Italian and US Families

Family Member	Mutation Carrier	Gender	Age (years)	Age at Diagnosis (years)	BMI (kg/m ²)	Glycemic Status	Current Treatment	FPG	PG 2 hr after OGTT	HbA1c (%)
Family: Italian										
III-1	yes	M	63	32	29.73	DM	ins	NA	NA	6.7
IV-1	yes	F	43	43	29.05	DM	diet	179	NA	7
IV-2	yes	F	39	–	31.59	NG	–	63	NA	4.5
IV-3	yes	F	48	48	32.81	PD	diet	92	NA	5.8
IV-4	yes	M	39	–	31.64	NG	–	86	74	NA
III-2	yes	M	59	50	29.41	DM	diet	153	NA	NA
IV-5	no	M	34	–	25.61	NG	–	91	81	3.7
IV-6	no	F	44	–	22.10	NG	–	95	108	3.8
III-6	yes	F	55	38	25.65	DM	ins	315	NA	NA
IV-7	yes	M	38	–	28.67	NG	–	78	NA	3.5
IV-8	yes	M	33	–	27.13	NG	–	98	121	3.8
IV-9	no	F	43	–	21.11	NG	–	77	NA	4.7
IV-10	yes	F	35	–	21.72	NG	–	81	NA	3.4
IV-11	yes	F	41	40	24.16	PD	diet	98	169	5.7
IV-12	no	F	37	–	29.30	NG	–	87	116	NA
III-7	no	F	56	–	26.64	NG	–	98	118	NA
IV-14	no	F	35	–	26.37	NG	–	86	119	5.6
IV-15	no	F	27	–	23.58	NG	–	76	75	NA
III-9	yes	M	52	46	27.94	DM	OHA	162	NA	NA
IV-16	no	F	32	–	34.77	NG	–	75	103	NA
IV-17	yes	F	24	–	25.77	NG	–	80	91	NA
IV-18	yes	M	30	–	28.41	NG	–	78	70	NA
III-12	yes	F	52	36	28.52	DM	ins	NA	NA	NA
IV-19	yes	M	35	–	24.93	NG	–	78	NA	3.2
IV-20	yes	F	39	–	24.17	NG	–	83	NA	5.2
III-14	yes	F	41	20	30.48	DM	ins	434	NA	NA
IV-21	yes	M	25	23	25.35	DM	OHA	252	NA	7.7
IV-22	yes	F	16	–	37.73	NG	–	86	NA	NA
Family: US										
II-3	no	M	75	–	27.26	NG	–	92	NA	NA
III-7	no	M	41	10	23.01	DM	ins	NA	NA	NA
II-5	yes	M	69	32	25.74	DM	ins	NA	NA	NA
III-1	no	F	52	–	40.76	NG	–	97	NA	NA
III-2	yes	M	49	48	27.33	DM	ins	NA	NA	NA
III-3	no	M	46	45	27.33	DM	ins	102	NA	6.4
III-4	no	F	47	–	22.05	NG	–	68	NA	5.4
IV-1	no	M	24	–	24.37	NG	–	75	NA	4.9
IV-2	no	M	20	–	23.01	NG	–	81	NA	5.1
III-5	yes	M	44	32	30.75	DM	ins	NA	NA	11.8

(Continued on next page)

Table 1. Continued

Family Member	Mutation Carrier	Gender	Age (years)	Age at Diagnosis (years)	BMI (kg/m ²)	Glycemic Status	Current Treatment	FPG	PG 2 hr after OGTT	HbA1c (%)
III-6	no	F	37	–	35.50	NG	–	95	NA	NA
III-8	yes	M	48	–	28.01	NG	–	72	62	5.4

Abbreviations are as follows: BMI, body mass index; DM, diabetes mellitus; FPG, fasting plasma glucose; HbA1c, glycated hemoglobin; ins, insulin; NA, not available; NG, normal glucose; OGTT, oral glucose tolerance test; OHA, oral antidiabetic agents; FPG, fasting plasma glucose; PD, pre-diabetes (as indicated by HbA1c \geq 5.7%, according to ADA criteria).

DNA samples extracted from peripheral blood by standard procedures; in the Italian families, a non-affected individual with age >50 years was also included in the study. All protein-coding regions, as defined by RefSeq 67, were targeted. About 210,000 coding exons were captured from 3 μ g of genomic DNA using the Agilent SureSelect Human All Exon v.4+UTRs, the Agilent SureSelect Human All Exon v.5, or the SeqCap EZ human Exome Library v.2.0 kit, according to the manufacturer's protocols. Whole-exome DNA libraries were sequenced on a HiSeq2000 (Illumina) in the US and a SOLID 5500XL (Life Technologies) in Italy. After mapping the short-reads to the GRCh37/hg19 human assembly by means of BWA⁸ and SAMtools⁹ or LifeScope (Life Technologies),¹⁰ variants were detected by means of GATK¹¹ and filtered to include only those with $\geq 5\times$ or $\geq 8\times$ depth of coverage as obtained by HiSeq or SOLID, respectively, and per-base and mapping quality phred values exceeding 30.

A total of 453,415 and 250,174 variants were identified in the US and Italian families, respectively (Table S1). Of these, 365,984 and 158,695, respectively, passed the primary QC filters. Homozygous variants, variants reported as validated polymorphisms with frequency >0.01 in publicly available human variation resources (dbSNP142, 1000 Genomes, NHLBI Exome Sequencing Project Exome Variant Server [EVS]), and variants not shared by both affected individuals were filtered out. Of the remaining variants, 7,972 and 644, respectively, were potentially deleterious, being nonsense, frameshift, or missense, or affecting splicing sites (Table S1). These variants were stratified through a mixed filtering/prioritization strategy taking into account the predicted impact of each variant¹² and the functional relevance of the corresponding genes with regard to diabetes. At the end of this process, described in detail in Figure S1, 35 variants in 28 genes and 4 variants in 3 genes were prioritized in the US and Italian datasets, respectively. The prioritized genes are listed in Table S2. One of them (*APPL1*, GenBank: NM_012096.2 and NP_036228.1) was present in both the Italian and US prioritization lists and, as such, was investigated further by Sanger sequencing and bioinformatic and functional studies. A nonsense mutation (c.1655T>A [p.Leu552*]) was identified in this gene in one of the Italian families whereas a missense substitution (c.280G>A [p.Asp94Asn]) was found in one of the US families (Figure S2). None of the other

prioritized variants were found in these two families. These other variants are being investigated by Sanger sequencing in the families in which they were originally identified to determine whether they segregate with diabetes according to an autosomal-dominant mode of inheritance.

Clinical features of the members of the two families with *APPL1* mutations are shown in Tables 1 and S3. In the Italian family, the p.Leu552* alteration was found in all the ten members with diabetes or pre-diabetes (Figure 1A). Eight of the individuals who did not have overt diabetes at examination (n = 19) did not have the mutation and the remaining were carriers (Figure 1A). Of note, most of the unaffected carriers were younger than 38 years (the median age at diabetes diagnosis among affected members) and were still at risk of developing diabetes in the future, especially considering that the presence of pre-diabetes could not be excluded in most of them due to the lack of oral glucose tolerance test (OGTT) data. It is also conceivable that the concomitant presence of a specific environment and/or other “modifier” genes is needed for this mutation to be fully penetrant—a scenario that has been observed for several human inherited diseases including familial diabetes.^{13–16} In this context, it is noteworthy that all non-affected subjects carrying the mutation belonged to the youngest generation. Although, in general, the environment has become more diabetogenic over the years, it is conceivable that, as compared to previous generations, young people from such heavily affected families might be paying more attention to a salutary lifestyle such as a proper diet and physical activity. This possibility is supported by the observation that in each affected subject of the youngest generation, diabetes was diagnosed at an older age (8 years on average) as compared to his/her affected parent.

In the US family, the p.Asp94Asn alteration was found or inferred to be present in five of the seven family members with diabetes (Figure 1B). One of the diabetic members who did not carry the mutation (III-7) had been diagnosed with type 1 diabetes at age 10; the other one (III-3) might have had the common, multifactorial form of type 2 diabetes, which is highly prevalent (12.3%) in the adult US population.¹⁷ A non-penetrant subject (III-8) was observed in the youngest generation also in this family (Figure 1B).

Both *APPL1* p.Asp94Asn and p.Leu552* alteration were not present in the database from the Exome

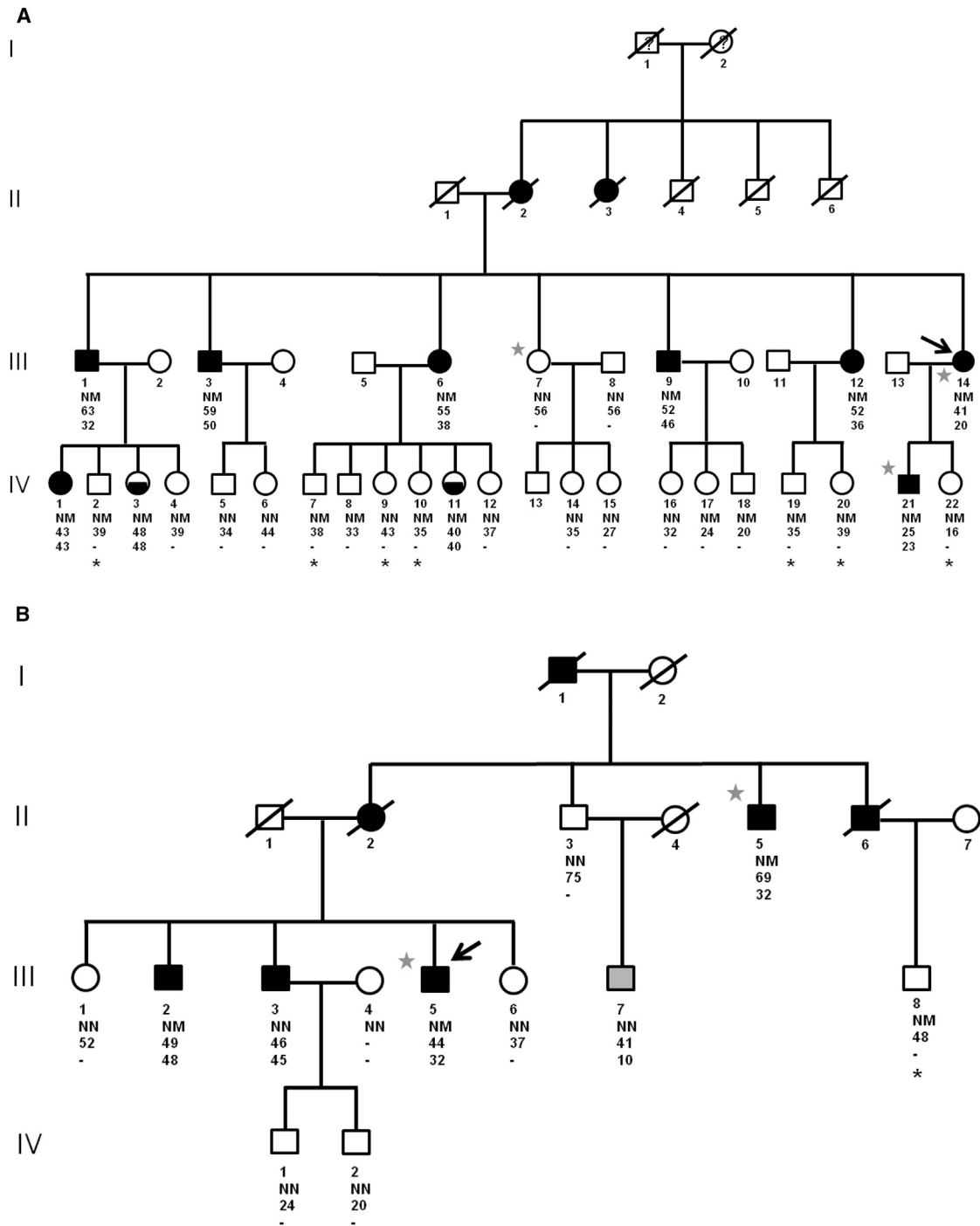


Figure 1. Pedigree Structures of the Two Families with *APPL1* Mutations

Shown are families from Italy (A) and from the US (B). Round and square symbols denote females and males, respectively. Filled and open symbols denote diabetic and non-diabetic subjects, respectively; half-filled symbols denote individuals with pre-diabetes (see definition in the text). The arrow points to the proband. Gray stars indicate family members in which WES was performed. Black stars indicate those individuals who did not undergo OGTT. Gray symbol denotes individual with type 1 diabetes. NM denotes presence of heterozygous *APPL1* mutations (p.Leu552* in the Italian family, p.Asp94Asn in the US family); NN denotes absence of such mutations. The age at examination is reported for each individual under the corresponding symbol; the age at diagnosis is reported for diabetic or prediabetic individuals under the age at examination.

Sequencing Project (EVS, n = 6,503) or in the larger Exome Aggregation Consortium database (ExAC, n = 61,486). In addition, we could not find either alteration among 1,639 non-diabetic and 2,970 T2D-affected unre-

lated individuals of European ancestry we previously described.¹⁸

No additional mutations were found by Sanger sequencing within the entire *APPL1* coding region

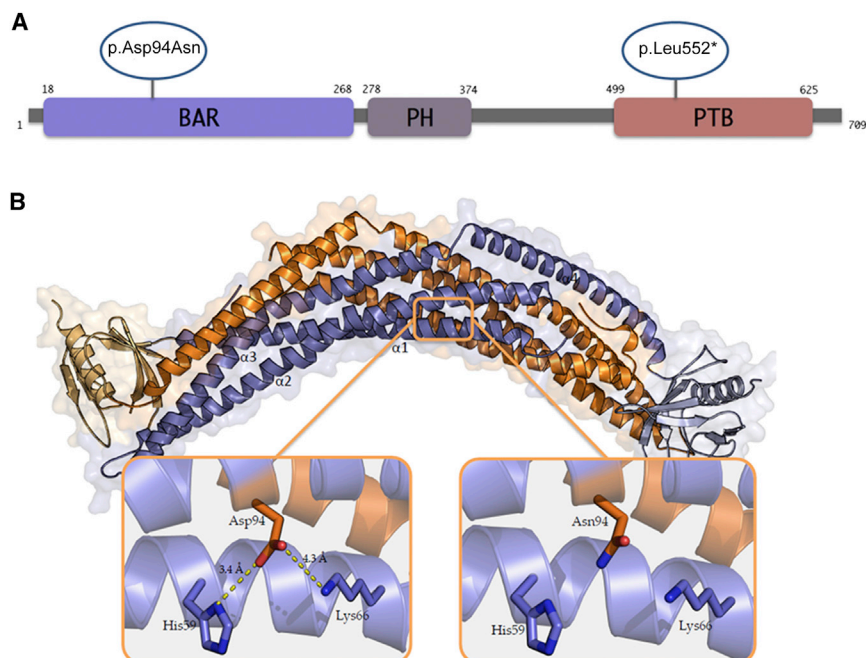


Figure 2. In Silico Prediction of the Effects of the Identified *APPL1* Mutations

(A) Schematic representation of the domains of the APPL1 protein and position of the identified alteration. Abbreviations are as follows: BAR, Bin/Amphiphysin/Rvs domain; PH, pleckstrin homology domain; PTB, phosphotyrosine-binding domain. Orange circles indicate the missense and the nonsense mutation at positions 94 and 552, respectively.

(B) Structure of the BAR-PH domain dimer of human APPL1 (PDB: 2Q13) and predicted effect of p.Asp94Asn alteration. One monomer is shown in orange, the other one in violet. The concave surface at the bottom is the lipid-binding surface enriched in positively charged residues, which is needed for the interaction with the plasma membrane. Asp94, located on the $\alpha 2$ helix, and the positively charged residues (His59 and Lys66), located on the $\alpha 1$ helix, are represented by sticks. Interactions and atomic distances between residues are visualized by yellow dashed lines. The substitution of the negatively charged amino acid Asp94 with a neutral one (Asn94) disrupts salt bridges with His59 and Lys66 (right). Inspection, measurement, and rendering were made with PyMOL software.

(consisting of 22 exons, Table S4) in the probands of 54 additional Italian kindreds with familial diabetes in which WES has not been performed yet.

APPL1 is an anchor protein consisting of 709 amino acids with multiple functional domains, including a Bin1/amphiphysin/rvs167 (BAR) domain, a pleckstrin homology (PH) domain, and a phosphotyrosine binding (PTB) domain¹⁹ (Figure 2A). As an adaptor protein, APPL1 interacts with several proteins including critical components of the insulin-signaling pathway.^{20–22} In agreement with this, several studies of mice models have clearly demonstrated a fundamental role for this protein in glucose homeostasis.^{20,21,23–25} Of particular importance in this regard is APPL1's interaction with AKT (MIM: 164731) in competition with the AKT endogenous inhibitor TRIB3 (MIM: 607898).²⁰ By virtue of its binding with APPL1 rather than TRIB3, AKT can be translocated to the plasma membrane, where it can be phosphorylated and activated, thereby propagating the insulin signal.^{21,22}

The nonsense *APPL1* alteration p.Leu552* is located in the PTB domain (aa 499–625, Figure 2A), which has been shown to bind the AKT catalytic domain.²⁶ The introduction of a premature stop codon at position 552 leads to the deletion of most of the PTB domain, thereby making APPL1 unable to bind AKT (Figure S3).

The missense mutation affects the aspartic acid residue at position 94 (i.e., Asp94), which resides on the concave surface of the APPL1 BAR domain (Figure 2) and is highly conserved among species (Figure S3). Sequence-based tools do not provide unequivocal answers about a pathogenic effect of an aspartic acid (Asp) to asparagine (Asn) substitu-

tion at this position. However, structure-based tools suggest that this mutation causes a protein structure destabilization that is likely to have functional consequences (Table S5). Structural and biochemical studies have shown that APPL proteins, including both APPL1 and its homolog APPL2 (MIM: 606231), are able to dimerize, forming homodimers (APPL1-APPL1 and APPL2-APPL2) as well as heterodimers (APPL1-APPL2).²⁷ All the homotypic and heterotypic APPL-APPL interactions are mediated by their BAR domains, which are also necessary for the association with curved cell membranes.^{27,28} The BAR dimer concave surface, lined with positively charged residues, is responsible for the interaction of this domain with the plasma membrane.^{29–32} In agreement with this, mutations localized to this surface have been reported to abolish APPL1 ability to bind the plasma membrane.^{33,34} The structural model of the APPL1 BAR domain (PyMOL) predicts that the substitution of a negatively charged amino acid (Asp94) with a neutral one (Asn94) disrupts salt bridges with residues His59 and Lys66 (Figure 3), thereby altering the BAR domain structural stability and possibly affecting its ability to dimerize as well as to bind the plasma membrane.

To evaluate the impact of the two *APPL1* mutations on insulin-mediated AKT activation and downstream signaling, APPL1 carrying the p.Leu552* or the p.Asp94Asn alteration were generated by site-directed mutagenesis of a pCMV6-Entry APPL1 myc tagged cDNA (Origene) and expressed in HepG2 cells (ATCC). These cells were chosen because they are (1) of human origin, (2) very insulin-responsive, and (3) isolated from liver, a central organ in the

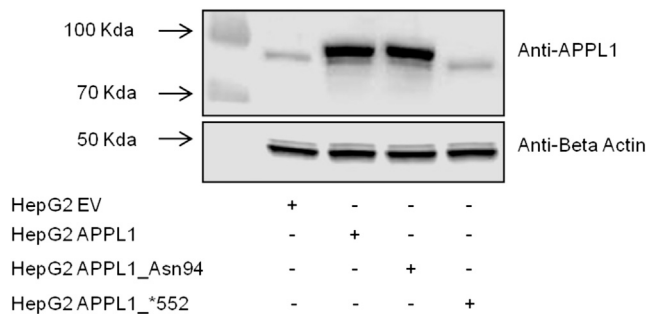


Figure 3. In Vitro Effects of the APPL1 Mutations on Protein Levels

HepG2 cells were transiently transfected with APPL1, APPL1_Asn94, APPL1_552, or empty vector (HEPG2_EV). After 48 hr transfection, cells were lysed and APPL1 and BETA ACTIN lower blot expression were evaluated by immunoblot analyses. In brief, equal amounts of protein from cell lysates were separated by SDS-PAGE and probed with anti-APPL1 (Cell Signaling) and anti-BETA ACTIN (Santa Cruz Biotechnology)-specific antibodies. A representative blot is shown.

maintenance of in vivo glucose homeostasis. Cells were kept at 37°C and 5% CO₂ in DMEM/F12 containing 10% FBS, were transiently transfected with APPL1 cDNA pCMV6 constructs carrying the wild-type sequence (HepG2 APPL1), the *552 alteration (HepG2 APPL1_552), or the Asn94 alteration (HepG2 APPL1_Asn94) by using TransIT reagent according to the manufacturer's instruc-

tions (Mirus). As compared to cells transfected with a control empty vector (HepG2_EV), cells transfected with any of the APPL1 cDNA constructs showed significant increase in APPL1 mRNA levels (as evaluated by quantitative RT-PCR), indicating that RNA stability was not negatively affected by these mutations (Table S6). In HepG2 APPL1 and APPL1_Asn94 cells, the mRNA increase was paralleled by an increase in APPL1 protein levels. By contrast, in HepG2 APPL1_552 cells, the APPL1 protein was almost undetectable, possibly due to instability and rapid degradation of the truncated protein (Figure 3). This result was confirmed with three different antibodies raised against three different APPL1 epitopes (data not shown). Given the lack of APPL1 protein expression caused by the p.Leu552* alteration, HepG2 APPL1_552 cells were not studied any further with regard to insulin signaling.

After insulin stimulation (100 nmol/l for 5 min) and cell lysis, equal amounts of protein were analyzed by immunoblot with specific antibodies against APPL1, phospho-AKT-S⁴⁷³, and phospho-GSK3β-S⁸ (Cell Signaling). The blots were then stripped and re-probed with antibodies against AKT and GSK3β (MIM: 605004; Cell Signaling) for normalization (Figure 4). In HepG2 APPL1 cells, insulin-induced AKT-S⁴⁷³ phosphorylation was increased by 47% as compared to HepG2_EV cells (p = 0.025) (Figure 4A). Such stimulatory effect of APPL1 was completely abolished by the Asn94 alteration (Figure 4A).

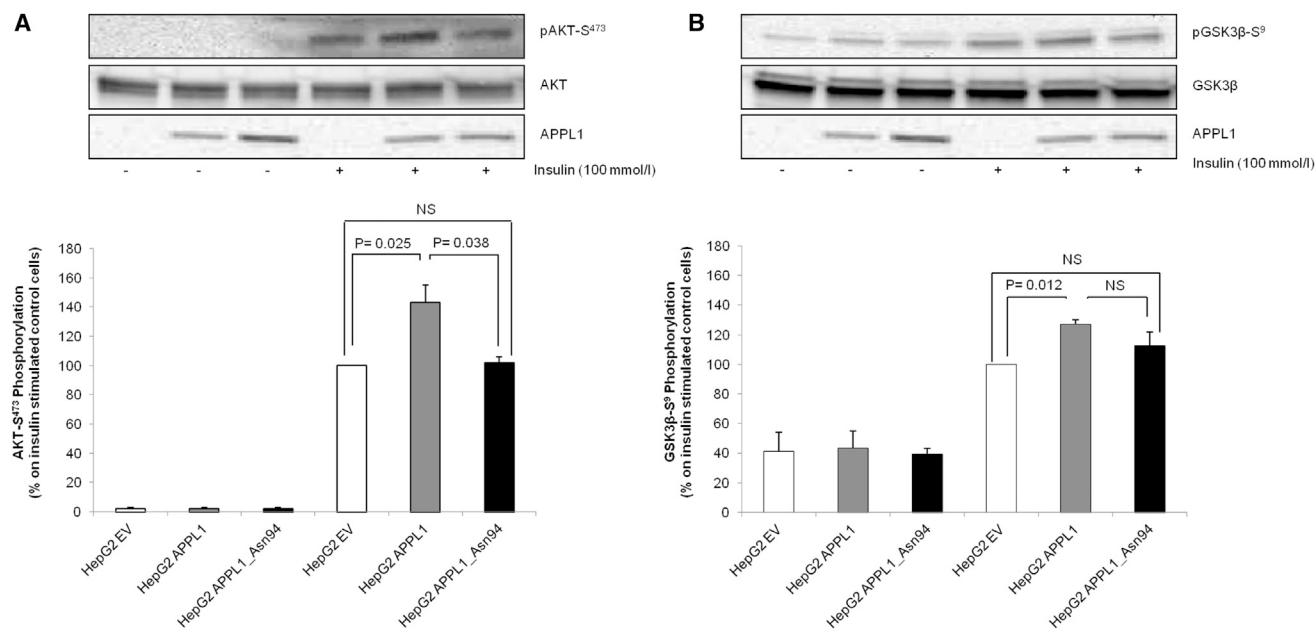


Figure 4. Effect of APPL1_Asn94 Transfection on Akt-S⁴⁷³ and GSK3β-S⁸ Phosphorylation

HepG2 cells were transiently transfected with APPL1, APPL1_Asn94, or empty vector. After 48 hr, cells were stimulated with 100 nmol/l insulin for 5 min and then lysed. Phospho-AKT-S⁴⁷³ (A) or phospho-GSK3β-S⁸ (B) were evaluated by immunoblot analyses. In brief, equal amount of protein from cell lysates were separated by SDS-PAGE and probed with anti-phospho-AKT-S⁴⁷³ (A, upper blot), anti-AKT (A, middle blot), anti-APPL1 (A and B, lower blot), or anti-phospho-GSK3β-S⁸ (B, upper blot) and anti-GSK3β (B, middle blot) specific antibodies, respectively. Gel images were acquired with Molecular Imager ChemiDoc XRS (Biorad) and analyzed with Kodak Molecular Imaging Software 4.0 or IMAGEJ 1.40 g (Wayne Rasband, NIH). A representative blot for each condition is shown. Bars represent the percentage of AKT-S⁴⁷³ phosphorylation/AKT OD ratio (A) or GSK3β-S⁸/GSK3β OD ratio (B) in insulin-stimulated control cells. Data are means ± SD of three experiments in separate times.

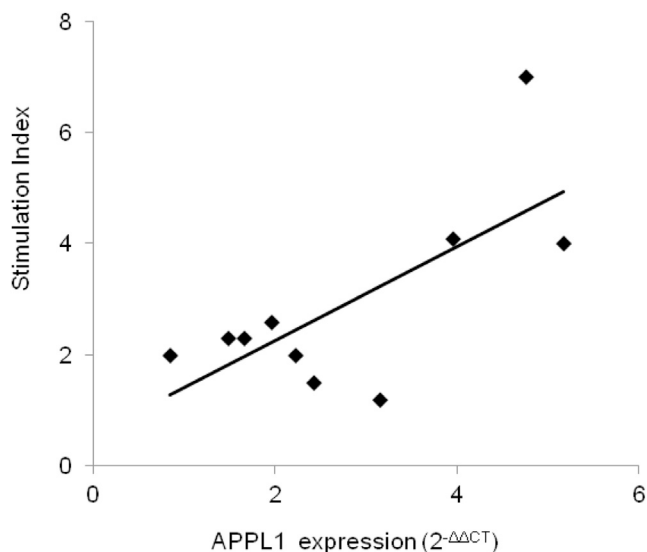


Figure 5. Correlation between APPL1 Expression and Glucose-Induced Insulin Secretion in Human Islets

Pancreata were collected from ten non-diabetic brain-dead multi-organ donors (age: 65.2 ± 13.6 years; 50% females) and pancreatic islets were prepared as previously described.³⁵ Glucose-induced insulin secretion was measured and then expressed as stimulation index (SI) calculated by dividing insulin release after glucose stimulation at 16.7 mmol/l over basal insulin release (i.e., at glucose 3.3 mmol/l). Prime Time Standard qPCR Assays (Integrated DNA Technologies) were used to quantify relative gene expression levels of *APPL1*, *GAPDH* (MIM: 138400), and *BETA ACTIN* (MIM: 102630) on ABI-PRISM 7900 (Applied Biosystems). *APPL1* expression was calculated by using the comparative $\Delta\Delta CT$ method. Relationship between SI and *APPL1* expression was evaluated by Pearson's correlation with SPSS 13 software. *APPL1* expression was significantly associated with SI ($r^2 = 0.50$, $p = 0.022$). This association remained significant also after adjusting for age and gender ($p = 0.048$).

Similarly, insulin-stimulated GSK3 β -S⁸ phosphorylation was increased by 27% in HepG2 APPL1 cells as compared to HepG2_EV cells ($p = 0.012$) (Figure 4B). In HepG2 APPL1_Asn94 cells, this effect was blunted to the extent that insulin-stimulated GSK3 β -S⁸ phosphorylation was no longer different from that in HepG2_EV control cells (Figure 4B).

Taken together, these results suggest that both p.Leu552* and p.Asp94Asn are loss-of-function alterations, one determining a complete lack of expression of the mutated allele, the other causing decreased functionality of a normally expressed allele. Given the central role of AKT in insulin signaling, these results support a detrimental role of both mutations on insulin action and, potentially, insulin secretion.

In mice, APPL1 is widely expressed in all insulin target tissues and organs including the liver, adipose tissue, skeletal muscle, and pancreas.²⁵ In the latter organ, the expression of APPL1 is higher in the islet than in the non-islet fraction (i.e., exocrine cells).²⁴ In islets, APPL1 co-localizes with insulin, indicating that this protein is abundantly expressed in β cells where it acts as a physiological regulator of insulin secretion.²⁴ Also in humans, APPL1 is expressed in all insu-

lin target tissues and organs (as reported by the public atlas of gene expression and regulation across multiple human tissues generated by The Genotype-Tissue Expression project [GTEx]). As in mice, APPL1 expression is particularly enriched in human islets (as reported by the T1Dbase-Beta Cell Gene Atlas), although no specific data on β cells are available. To obtain further insights about the role of APPL1 on insulin secretion in humans, we measured APPL1 expression levels and glucose-induced insulin secretion in human islets from ten brain-dead multi-organ donors (five males, five females; BMI range: 19.4–34.8 kg/m²). None of the donors were diabetic, as indicated by the medical records obtained from the intensive care units (ICUs). Mean glucose levels under continuous glucose infusion in the ICU ranged from 63 to 192 mg/dl. Fructosamine levels were available for five out of ten individuals and ranged from 105 to 278 $\mu\text{mol/l}$ (reference values for non-diabetic individuals: $<285 \mu\text{mol/l}$). APPL1 expression was significantly correlated with glucose-induced insulin secretion (Figure 5), suggesting that the positive role of APPL1 on insulin secretion reported in rodents^{23–25} is also operating in humans and reinforcing the possibility that human mutations reducing APPL1 expression levels or its function in insulin signaling might affect not only insulin sensitivity but also insulin secretion.

In conclusion, this study describes *APPL1* mutations as pathogenic factors for familial forms of diabetes. This finding is consistent with previous evidence from animal studies supporting a key regulatory role of APPL1 in glucose metabolism and points to this molecule as a potential target for future treatments aimed at preserving or restoring glucose homeostasis.

Supplemental Data

Supplemental Data include four figures and six tables and can be found with this article online at <http://dx.doi.org/10.1016/j.ajhg.2015.05.011>.

Acknowledgments

We wish to thank the subjects and families involved in the study. This work was supported by the Italian Society of Diabetology (SID) (grant FO.RI.SID 2011 to S. Prudente), NIH (grant R01DK55523 to A.D. and P30 DK036836 to the Joslin Diabetes Research Center [Advanced Genomics and Genetics Core]), and the Italian Ministry of Health (Ricerca Corrente 2014 and 2015 to S. Prudente, R.D.P., and V.T.).

Received: March 2, 2015

Accepted: May 14, 2015

Published: June 11, 2015

Web Resources

The URLs for data presented herein are as follows:

1000 Genomes, <http://browser.1000genomes.org>

Clustal Omega, <http://www.ebi.ac.uk/Tools/msa/clustalo/>

CUPSAT, <http://cupsat.tu-bs.de>
 dbSNP, <http://www.ncbi.nlm.nih.gov/projects/SNP/>
 Diabetes Atlas, <http://www.idf.org/diabetesatlas>
 ExAC Browser, <http://exac.broadinstitute.org/>
 GTEx Portal, <http://www.gtportal.org/home/>
 I-Mutant, <http://folding.biofold.org/i-mutant/i-mutant2.0.html>
 LifeScope, <http://www.lifetechnologies.com/lifescopelife>
 MUPRO, <http://mupro.proteomics.ics.uci.edu>
 Mutation Assessor, <http://mutationassessor.org/>
 MutationTaster, <http://www.mutationtaster.org/>
 NHLBI Exome Sequencing Project (ESP) Exome Variant Server, <http://evs.gs.washington.edu/EVS/>
 OMIM, <http://www.omim.org/>
 PolyPhen-2, <http://www.genetics.bwh.harvard.edu/pph2/>
 PyMOL, <http://www.pymol.org>
 RCSB Protein Data Bank, <http://www.rcsb.org/pdb/home/home.do>
 RefSeq, <http://www.ncbi.nlm.nih.gov/RefSeq>
 SIFT, <http://sift.bii.a-star.edu.sg/>
 T1DBase, <https://www.t1dbase.org>
 WebLogo 3, <http://weblogo.threeplusone.com>

References

- Roglic, G., Unwin, N., Bennett, P.H., Mathers, C., Tuomilehto, J., Nag, S., Connolly, V., and King, H. (2005). The burden of mortality attributable to diabetes: realistic estimates for the year 2000. *Diabetes Care* 28, 2130–2135.
- Vaxillaire, M., and Froguel, P. (2008). Monogenic diabetes in the young, pharmacogenetics and relevance to multifactorial forms of type 2 diabetes. *Endocr. Rev.* 29, 254–264.
- Schwitzgebel, V.M. (2014). Many faces of monogenic diabetes. *J. Diabetes Investig.* 5, 121–133.
- Bamshad, M.J., Ng, S.B., Bigham, A.W., Tabor, H.K., Emond, M.J., Nickerson, D.A., and Shendure, J. (2011). Exome sequencing as a tool for Mendelian disease gene discovery. *Nat. Rev. Genet.* 12, 745–755.
- Doria, A., Yang, Y., Malecki, M., Scotti, S., Dreyfus, J., O’Keeffe, C., Orban, T., Warram, J.H., and Krolewski, A.S. (1999). Phenotypic characteristics of early-onset autosomal-dominant type 2 diabetes unlinked to known maturity-onset diabetes of the young (MODY) genes. *Diabetes Care* 22, 253–261.
- Kim, S.H., Warram, J.H., Krolewski, A.S., and Doria, A. (2001). Mutation screening of the neurogenin-3 gene in autosomal dominant diabetes. *J. Clin. Endocrinol. Metab.* 86, 2320–2322.
- Fajans, S.S., and Bell, G.I. (2011). MODY: history, genetics, pathophysiology, and clinical decision making. *Diabetes Care* 34, 1878–1884.
- Li, H., and Durbin, R. (2010). Fast and accurate long-read alignment with Burrows-Wheeler transform. *Bioinformatics* 26, 589–595.
- Li, H., Handsaker, B., Wysoker, A., Fennell, T., Ruan, J., Homer, N., Marth, G., Abecasis, G., and Durbin, R.; 1000 Genome Project Data Processing Subgroup (2009). The Sequence Alignment/Map format and SAMtools. *Bioinformatics* 25, 2078–2079.
- Castellana, S., Romani, M., Valente, E.M., and Mazza, T. (2013). A solid quality-control analysis of AB SOLiD short-read sequencing data. *Brief. Bioinform.* 14, 684–695.
- McKenna, A., Hanna, M., Banks, E., Sivachenko, A., Cibulskis, K., Kernysky, A., Garimella, K., Altshuler, D., Gabriel, S., Daly, M., and DePristo, M.A. (2010). The Genome Analysis Toolkit: a MapReduce framework for analyzing next-generation DNA sequencing data. *Genome Res.* 20, 1297–1303.
- Castellana, S., and Mazza, T. (2013). Congruency in the prediction of pathogenic missense mutations: state-of-the-art web-based tools. *Brief. Bioinform.* 14, 448–459.
- Cooper, D.N., Krawczak, M., Polychronakos, C., Tyler-Smith, C., and Kehrer-Sawatzki, H. (2013). Where genotype is not predictive of phenotype: towards an understanding of the molecular basis of reduced penetrance in human inherited disease. *Hum. Genet.* 132, 1077–1130.
- Bonnefond, A., Philippe, J., Durand, E., Dechaume, A., Huyvaert, M., Montagne, L., Marre, M., Balkau, B., Fajardy, I., Vambergue, A., et al. (2012). Whole-exome sequencing and high throughput genotyping identified KCNJ11 as the thirteenth MODY gene. *PLoS ONE* 7, e37423.
- Meur, G., Simon, A., Harun, N., Virally, M., Dechaume, A., Bonnefond, A., Fetita, S., Tarasov, A.I., Guillausseau, P.J., Boesgaard, T.W., et al. (2010). Insulin gene mutations resulting in early-onset diabetes: marked differences in clinical presentation, metabolic status, and pathogenic effect through endoplasmic reticulum retention. *Diabetes* 59, 653–661.
- Edghill, E.L., Flanagan, S.E., Patch, A.M., Bousted, C., Parrish, A., Shields, B., Shepherd, M.H., Hussain, K., Kapoor, R.R., Malecki, M., et al.; Neonatal Diabetes International Collaborative Group (2008). Insulin mutation screening in 1,044 patients with diabetes: mutations in the INS gene are a common cause of neonatal diabetes but a rare cause of diabetes diagnosed in childhood or adulthood. *Diabetes* 57, 1034–1042.
- Centers for Disease Control and Prevention; National Diabetes Statistics Report (2014). Estimates of Diabetes and Its Burden in the United States, 2014 (Atlanta: U.S. Department of Health and Human Services).
- Prudente, S., Morini, E., Marselli, L., Baratta, R., Copetti, M., Mendonca, C., Andreozzi, F., Chandalia, M., Pellegrini, F., Balletti, D., et al. (2013). Joint effect of insulin signaling genes on insulin secretion and glucose homeostasis. *J. Clin. Endocrinol. Metab.* 98, E1143–E1147.
- Deepa, S.S., and Dong, L.Q. (2009). APPL1: role in adiponectin signaling and beyond. *Am. J. Physiol. Endocrinol. Metab.* 296, E22–E36.
- Saito, T., Jones, C.C., Huang, S., Czech, M.P., and Pilch, P.F. (2007). The interaction of Akt with APPL1 is required for insulin-stimulated Glut4 translocation. *J. Biol. Chem.* 282, 32280–32287.
- Ryu, J., Galan, A.K., Xin, X., Dong, F., Abdul-Ghani, M.A., Zhou, L., Wang, C., Li, C., Holmes, B.M., Sloane, L.B., et al. (2014). APPL1 potentiates insulin sensitivity by facilitating the binding of IRS1/2 to the insulin receptor. *Cell Rep.* 7, 1227–1238.
- Prudente, S., Sesti, G., Pandolfi, A., Andreozzi, F., Consoli, A., and Trischitta, V. (2012). The mammalian tribbles homolog TRIB3, glucose homeostasis, and cardiovascular diseases. *Endocr. Rev.* 33, 526–546.
- Cheng, K.K., Iglesias, M.A., Lam, K.S., Wang, Y., Sweeney, G., Zhu, W., Vanhoutte, P.M., Kraegen, E.W., and Xu, A. (2009). APPL1 potentiates insulin-mediated inhibition of hepatic glucose production and alleviates diabetes via Akt activation in mice. *Cell Metab.* 9, 417–427.
- Wang, C., Li, X., Mu, K., Li, L., Wang, S., Zhu, Y., Zhang, M., Ryu, J., Xie, Z., Shi, D., et al. (2013). Deficiency of APPL1 in mice impairs glucose-stimulated insulin secretion through inhibition of pancreatic beta cell mitochondrial function. *Diabetologia* 56, 1999–2009.

25. Han, W. (2012). Dual functions of adaptor protein, phosphotyrosine interaction, PH domain and leucine zipper containing 1 (APPL1) in insulin signaling and insulin secretion. *Proc. Natl. Acad. Sci. USA* *109*, 8795–8796.
26. Mitsuuchi, Y., Johnson, S.W., Sonoda, G., Tanno, S., Golemis, E.A., and Testa, J.R. (1999). Identification of a chromosome 3p14.3-21.1 gene, APPL, encoding an adaptor molecule that interacts with the oncoprotein-serine/threonine kinase AKT2. *Oncogene* *18*, 4891–4898.
27. Chial, H.J., Wu, R., Ustach, C.V., McPhail, L.C., Mobley, W.C., and Chen, Y.Q. (2008). Membrane targeting by APPL1 and APPL2: dynamic scaffolds that oligomerize and bind phosphoinositides. *Traffic* *9*, 215–229.
28. Chial, H.J., Lenart, P., and Chen, Y.Q. (2010). APPL proteins FRET at the BAR: direct observation of APPL1 and APPL2 BAR domain-mediated interactions on cell membranes using FRET microscopy. *PLoS ONE* *5*, e12471.
29. Li, J., Mao, X., Dong, L.Q., Liu, F., and Tong, L. (2007). Crystal structures of the BAR-PH and PTB domains of human APPL1. *Structure* *15*, 525–533.
30. Masuda, M., and Mochizuki, N. (2010). Structural characteristics of BAR domain superfamily to sculpt the membrane. *Semin. Cell Dev. Biol.* *21*, 391–398.
31. Suetsugu, S., Toyooka, K., and Senju, Y. (2010). Subcellular membrane curvature mediated by the BAR domain superfamily proteins. *Semin. Cell Dev. Biol.* *21*, 340–349.
32. Mim, C., and Unger, V.M. (2012). Membrane curvature and its generation by BAR proteins. *Trends Biochem. Sci.* *37*, 526–533.
33. Peter, B.J., Kent, H.M., Mills, I.G., Vallis, Y., Butler, P.J., Evans, P.R., and McMahon, H.T. (2004). BAR domains as sensors of membrane curvature: the amphiphysin BAR structure. *Science* *303*, 495–499.
34. Wu, T., Shi, Z., and Baumgart, T. (2014). Mutations in BIN1 associated with centronuclear myopathy disrupt membrane remodeling by affecting protein density and oligomerization. *PLoS ONE* *9*, e93060.
35. Marchetti, P., Bugliani, M., Lupi, R., Marselli, L., Masini, M., Boggi, U., Filipponi, F., Weir, G.C., Eizirik, D.L., and Cnop, M. (2007). The endoplasmic reticulum in pancreatic beta cells of type 2 diabetes patients. *Diabetologia* *50*, 2486–2494.

The American Journal of Human Genetics

Supplemental Data

Loss-of-Function Mutations

in *APPL1* in Familial Diabetes Mellitus

Sabrina Prudente, Prapaporn Jungtrakoon, Antonella Marucci, Ornella Ludovico, Patinut Buranasupkajorn, Tommaso Mazza, Timothy Hastings, Teresa Milano, Eleonora Morini, Luana Mercuri, Diego Bailetti, Christine Mendonca, Federica Alberico, Giorgio Basile, Marta Romani, Elide Miccinilli, Antonio Pizzuti, Massimo Carella, Fabrizio Barbetti, Stefano Pascarella, Piero Marchetti, Vincenzo Trischitta, Rosa Di Paola, and Alessandro Doria

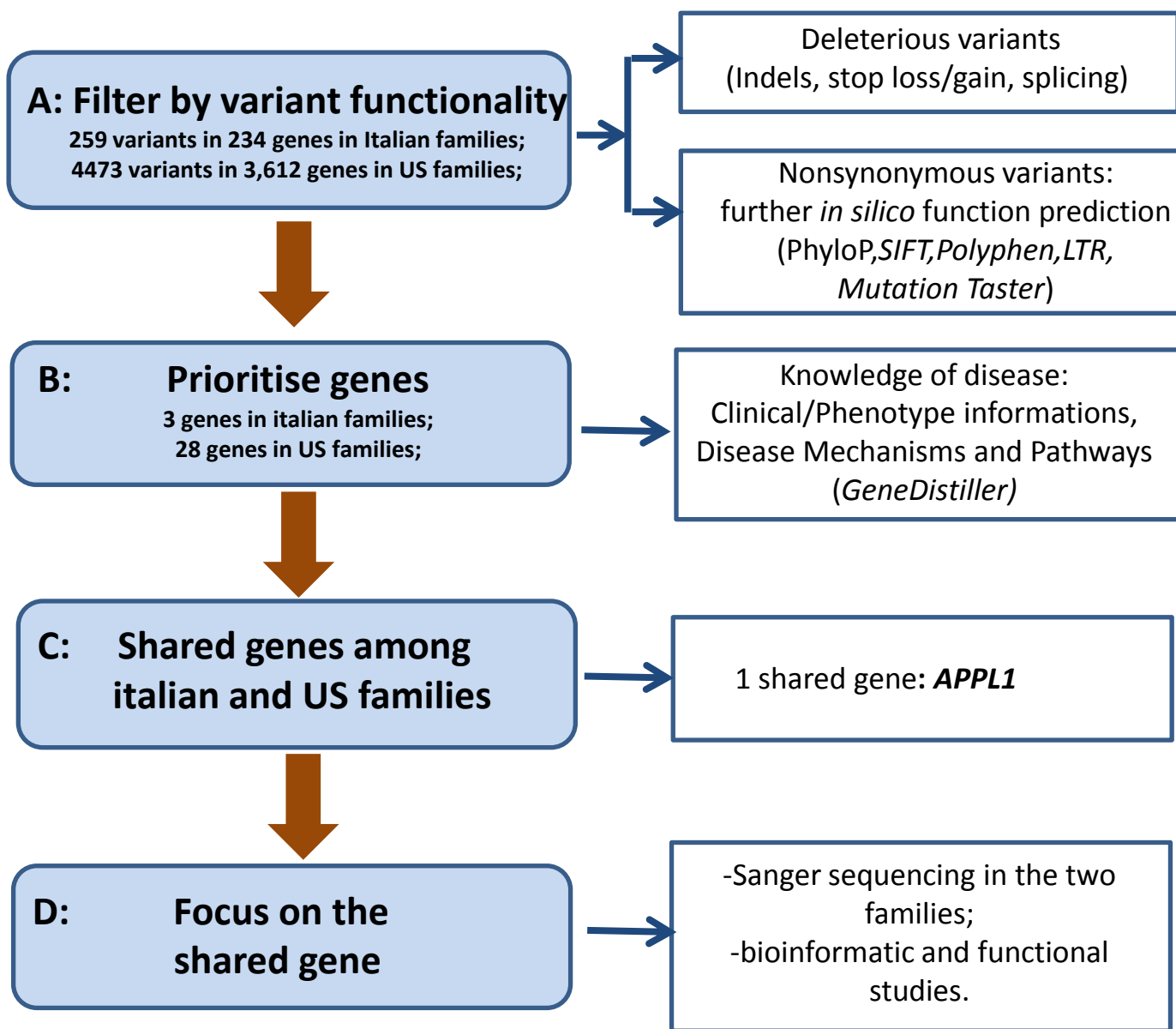


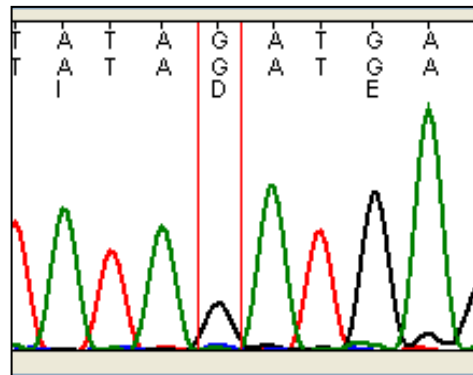
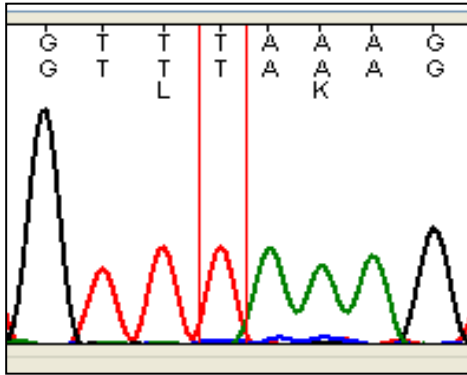
Figure S1. Strategy to filter and prioritize candidate variants in the Italian and US families.

Candidate variants were stratified through a mixed filtering/prioritization strategy taking into account the predicted impact of each variant and the functional relevance of individual genes with regard to the disease of interest (i.e. diabetes mellitus). In Step A, variants were filtered by functionality and only changes in residues conserved among species (as evaluated by PhyloP) or predicted to be deleterious by at least of one of four different prediction algorithms (i.e., SIFT, PolyPhen2, LRT and MutationTaster) or “inapplicable” by any predictors were retained. Variants identified in Step A were prioritized in Step B on the basis of the functional relevance of the genes in which they occurred using “GeneDistiller” (Seelow D et al., PLoS ONE 2008; 3:e3874). Genes were ranked based on combinations of terms based on knowledge of disease (including clinical and phenotype information, disease mechanisms and pathways) including non-insulin dependent diabetes mellitus (NIDDM) maturity onset diabetes of the young (MODY), permanent neonatal diabetes mellitus (PNDM), insulin, glucose, pancreas and islets as keywords in the OMIM entries, and using similarity of expression patterns, protein-protein interactions, and specific tissues expression (i.e. liver, pancreatic islets, adipocytes and skeletal muscle) as major weights. By using these filtering criteria, 4 variants in 3 genes and 35 variants in 28 genes were prioritized in the Italian and the US sets, respectively. We focused the present study on the only gene (*APPL1*) that was shared by the two prioritization lists.

A Individuals from Italian family

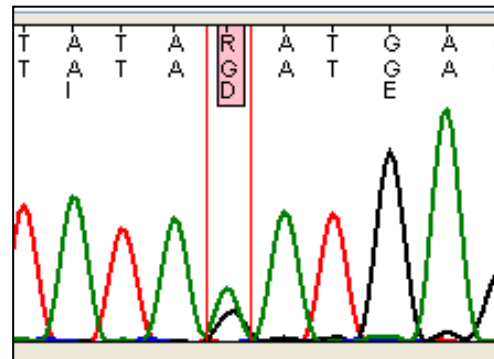
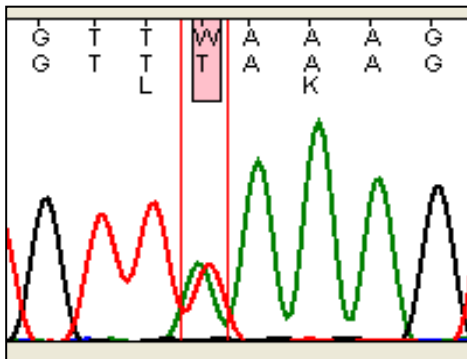
B Individuals from US family

Wild type



Wild type

Mutated



Mutated

Figure S2. Electropherograms of the *APPL1* mutations identified in two families.

The panel A shows the heterozygous non-sense mutation c.1655T>A: p.Leu552* (marked with an arrow) in exon 17 found in the Italian family.

The panel B shows the heterozygous missense mutation c.280G>A: p.Asp94Asn (marked with an arrow) in exon 4 found in the family from US.

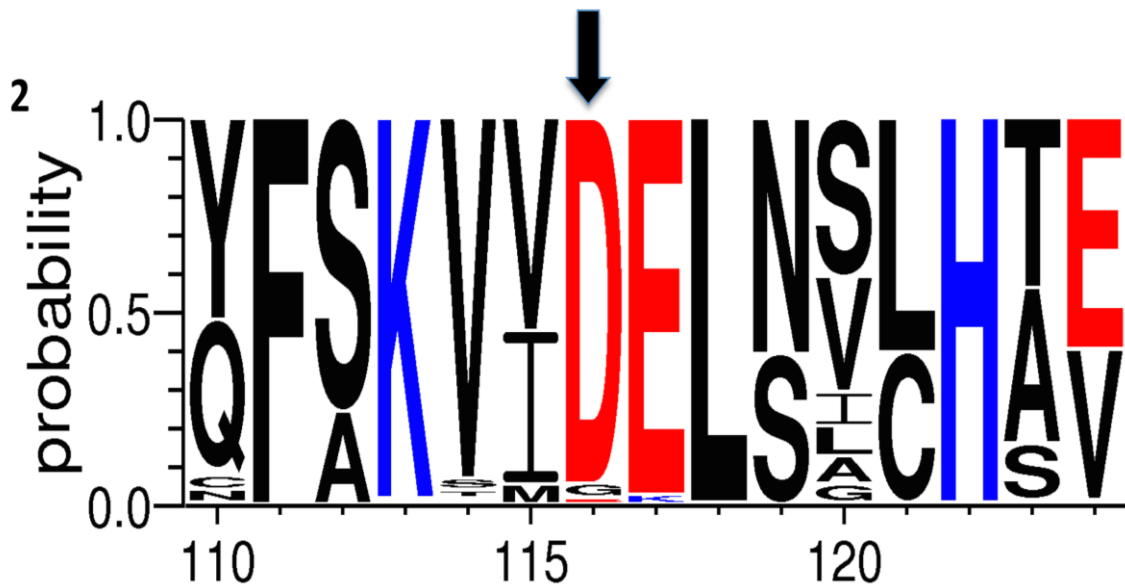


Figure S3. Aminoacid conservation in the APPL1 region encompassing Asp94

Multiple-sequence alignment of the APPL1 BAR domain from 244 homologous sequences was performed with the Clustal Omega sequence-alignment tool. Logo was calculated by means of the WebLogo service. The height of each amino acid one-letter code is proportional to the observed frequency of the residue at that position.

Numbering refers to the alignment.

Asp94 (indicated by the black arrow) appears to be highly conserved.

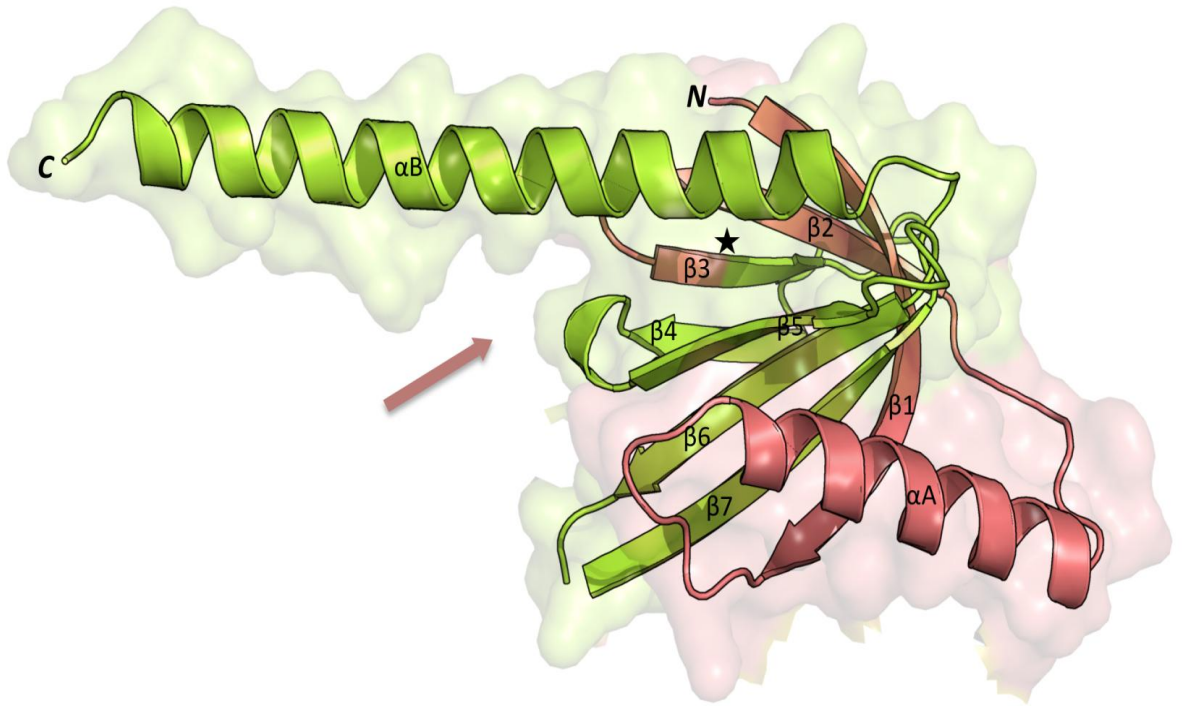


Figure S4. Structure of the PTB domain of human APPL1.

Phosphotyrosine binding domain (PTB) of human APPL1 (Protein Data Bank ID: 2ELA) is represented. The star denotes the position of Leu552 in the third β -sheet of PTB domain: the premature stop codon results in a deletion of the protein structure shown in green, while the region before the mutation is coloured in magenta. The arrow indicates the peptide-binding site (between β 5 sheet and C-terminal helix) in most of the proteins containing PTB domain.

Table S1. Summary of whole-exome sequencing (WES) performance in US and Italian families

	Variants (N)	
	Italian families (n=8)	US families (n=52)
Individuals subjected to WES	24	104
All variants	250,174	453,415
Passing primary QC filters	158,695	365,984
Heterozygous	92,043	214,118
Novel, infrequent or rare (MAF <0.01)	14,726	133,742
Shared by two affected members	3,109	30,107
Nonsense, frameshift, missense, splicing	644	7,972

Table S2. Candidate disease genes obtained after prioritization in both the Italian and US families

Italian Families			US Families		
Gene	Gene ID	Gene Distiller Overall Score	Gene	Gene ID	Gene Distiller Overall Score
APPL1	26060	5898	<i>GCG</i>	2641	68431
<i>CPT1A</i>	1374	5548	<i>ADIPOQ</i>	9370	31117
<i>TRIB3</i>	57761	271	<i>MAPK3</i>	5595	26747
			<i>SREBF1</i>	6720	26410
			<i>GLP1R</i>	2740	24728
			<i>PTPN1</i>	5770	20433
			<i>G6PC2</i>	57818	20359
			<i>PTPN11</i>	5781	19198
			<i>AKT2</i>	208	16489
			<i>FOXA1</i>	3169	12469
			<i>STXBP4</i>	252983	11239
			<i>PRKAA2</i>	5663	8656
			<i>TSC2</i>	7241	7312
			<i>ITPR3</i>	3710	7277
			<i>SORBS1</i>	10580	6141
			APPL1	26060	5848
			<i>MET</i>	4233	4107
			<i>RAPGEF4</i>	11069	3845
			<i>KL</i>	9365	3362
			<i>ANKRD26</i>	22852	3063
			<i>PRKAR1B</i>	5575	2460
			<i>PRKAG3</i>	53632	2320
			<i>MTOR</i>	2474	236
			<i>ADRA2</i>	150	98
			<i>WFS1</i>	7466	89
			<i>CACNAE1</i>	777	41
			<i>RFX6</i>	222546	22
			<i>ASPSCR1</i>	79058	21

Genes prioritization has been carried out by «GeneDistiller» <http://www.genedistiller.org>

Table S3. Average clinical features of examined members from Italian and US families according to their genetic and glycemc status.

Family	Status	Gender (M/F)	Age	Age at diagnosis	BMI	FPG
<i>Italian</i>	Non affected subjects (non carriers)	1/7	38.5±8.9	-	26.2±4.4	85.6±8.9
	Non affected subjects (carriers)	5/5	32.8±7.6	-	28.2±4.6	81.1±8.8
	Affected subjects (carriers)	4/6	47.9±10.9	37.6±10.1	28.3±2.5	-
<i>US</i>	Non affected subjects (non carriers)	3/3	42.5±20.2	-	28.8±7.6	84.7±11.8
	Non affected subjects (carriers)	1	48.0	-	28.0	72.0
	Affected subjects* (carriers)	3/0	54.0±13.2	37.33±9.2	27.9±2.6	-

BMI: body mass index; FPG: fasting plasma glucose;

*this group comprises neither the patient with type 1 diabetes nor the one with type 2 diabetes who does not carry mutation.

Table S4. Primers and PCR conditions used for *APPL1* gene (NC_000003.12 57227737..57273471) resequencing

Primer Name	Primer sequence	Length	Ta	Product Size
APPL1-Ex1-F	ACGGTCCCCTGCGATTTAG	19	59	590
APPL1-Ex1-R	CCCAGCCTCCACAACCTCC	18		
APPL1-Ex2-F	TTGGAAAATACCTCTGCTTTG	21	53	531
APPL1-Ex2-R	ATGCTTCAATCGTCTATCACTTT	23		
APPL1-Ex3-F	GGCAATAATCAGTCATCAACG	21	53	645
APPL1-Ex3-R	GCTCCAGTTCCTCCAATAACAC	22		
APPL1-Ex4-F	GCTGTGACTTGCTGAACATTAC	22	53	632
APPL1-Ex4-R	TCTTCTCTCCCTGCCTACATC	21		
APPL1-Ex5-F	TGTTCCCTTGCTTTTAGTGCA	23	53	474
APPL1-Ex5-R	TCCTATAAATGTTTGTAAGTGAAGC	25		
APPL1-Ex6-F	CAGAGTAGCTTTTTACCCCTGA	22	63	579
APPL1-Ex6-R	GGGCAGCAGGATCACTACA	19		
APPL1-Ex7-F	TTCAAGCCACAATCATAGCATACT	23	53	702
APPL1-Ex7-R	TCAAAATACAAAGCAACAAAAGG	23		
APPL1-Ex8-F	TTCTAAAAGATCAGAAAACAGGAACA	26	53	496
APPL1-Ex8-R	TGCAAGGAAAACCATTCTTC	20		
APPL1-Ex9-F	TCCTTAATGGCTCCCTGTGCAGT	23	53	495
APPL1-Ex9-R	TCCCATCAAACCTCCACAATTTCA	24		
APPL1-Ex10-F	CCCATGCCGCTCTTCCTCTC	20	68	524
APPL1-Ex10-R	ATGCCCAGCCCTGGTTTCAC	20		
APPL1-Ex11-F	ATTTCCAGCCTTGTTTTGG	19	53	671
APPL1-Ex11-R	AGGATTTTCAGTTCAGTTCC	21		
APPL1-Ex12-F	TGAGGATCAGCACCTGTTCCCTT	23	53	572
APPL1-Ex12-R	CAGCCTGCCAGACAGCAACA	20		
APPL1-Ex13-F	TGCAGTTGAGTATTGAACATTTGCCT	20	64	534
APPL1-Ex13-R	TCATGGCACATTAAGCTACTCATTCA	20		
APPL1-Ex14-15-F	CAACACTTGCAGGGAATTTT	20	53	811
APPL1-Ex14-15-R	GAAATGCAGACAGGGGATTA	20		
APPL1-Ex16-F	AGGATGGGGCATTTTAGAGC	20	63	560
APPL1-Ex16-R	CACACAAACACACAACAACCTGG	22		
APPL1-Ex17-18-F	GAAAACCTAAAAGGAGGCAGTG	22	53	554
APPL1-Ex17-18-R	CAGCCAAAGACCAATCATAGC	21		
APPL1-Ex19-F	TTCAACAACCTTTTTCTGCTTG	22	53	558
APPL1-Ex19-R	TTGGATGATGGACACCCTAAA	21		
APPL1-Ex20-F	AGGTGAGAGTCAGCAGTGGA	21	64	479
APPL1-Ex20-R	CAAGTCATTCTCGTGCCTCA	20		
APPL1-Ex21-F	GATGCTTGATTTTCCAAGAATG	22	53	500
APPL1-Ex21-R	TCTGTTTATGAAGTGGCTGAAC	22		
APPL1-Ex22-F	TGGTGTGTATTGTTGGGTGT	22	53	583
APPL1-Ex22-R	GAGCAAATGTAATTCCTCAGCA	22		

Table S5. Software prediction algorithms used to assess the Asp94Asn mutation effect on APPL1 protein

Software prediction algorithm	Score	Effect predicted
<i>Sequence based</i>		
SIFT	0.37(cutoff = 0.05)	Neutral
Polyphen-2	0.61(scale 0 to 1)	Possibly damaging
Panther	0.66 (scale 0 to 1)	Deleterious
<i>Structure based</i>		
CUPSAT	$\Delta\Delta G = -0.22$ kcal/mol	Overall stability = Destabilising Torsion angles = Unfavourable
I-Mutant 2.0	$\Delta\Delta G = -1.30$ kcal/mol	Decrease stability
MUPRO	Confidence score = -0.96 (scale -1 to 1, -1 = max. decrease stability)	Decrease stability

Table S6. APPL1 mRNA expression levels in transfected HepG2 cells.

	APPL1 expression levels ($2^{-\Delta\Delta CT} \pm sd$)
HepG2 EV	1
HepG2 APPL1	1048 \pm 173
HepG2 APPL1_X552	1003 \pm 108
HepG2 APPL1_ASN94	1135 \pm 144

HepG2 EV: HepG2 cells transiently transfected with control empty vector.

HepG2 APPL1: HepG2 cells transiently transfected with pCMV6-Entry APPL1 myc tagged cDNA.

HepG2 APPL1_X552: HepG2 cells transiently transfected with APPL1 cDNA carrying X552 mutation.

HepG2 APPL1_ASN94: HepG2 cells transiently transfected with APPL1 cDNA carrying ASN94 mutation.

RNA was isolated by using RNeasy Mini kit (Qiagen S.r.l., Milan, Italy), cDNA generated by reverse transcription with iScript Reverse Transcription (Biorad, Hercules, CA) according to the manufacturer's instructions and used as template in the subsequent analyses. Prime Time Std qPCR Assays (IDT, Iowa USA) were used to quantify relative gene expression levels of APPL1, GAPDH, B actin and 18S on ABI-PRISM 7900 (Applied Biosystems, Carlsbad, CA). Expression levels of APPL1 across different experimental conditions were calculated by using the comparative ΔCT method. Briefly, the amount of APPL1 was normalized to the geometric mean of GAPDH, B actin and 18S expression and related to APPL1 expression in HepG2 EV control cells ($2^{-\Delta\Delta CT}$). Data are presented as $2^{-\Delta\Delta CT} \pm sd$.